HiSST: 3rd International Conference on High-Speed Vehicle Science Technology

14 -19 April 2024, Busan, Korea

CMCs for missile applications: elaboration and NDT of EBCs at an industrial scale

RAYNAUD Jonathan[1], LHUISSIER Maxime[1], ROLLIN Magali[1]

Abstract

Ceramic matrix composites (CMCs) are used in high temperature applications, for example for aircraft brakes or rocket nozzles. In recent years, this kind of materials is of more and more interest for the development of missile parts subjected to temperatures above 400 °C.

To guarantee their performances, some CMCs require to be protected by an environmental barrier coating (EBC). Despite their low thickness which do not exceed a few hundred microns, an EBC has to avoid air penetration in the CMC structure. So, it has to contain a minimum amount of microcracks and pores. Firstly, this needs an adapted elaboration process, robust whatever the dimensions and the shape of the parts. Secondly, this needs control methods able to visualize the microstructure non-destructively with a sufficient resolution.

EBCs have been elaborated at the surface of a C/C plate by several technics using the same principle: application of a slurry, drying and heating. These technics are Liquid Silicium Infiltration (LSI) and Polymer Derived Ceramic (PDC). Some process parameters have been studied to know their influence on the EBC microstructure: CMC surface roughness, slurry coating thickness, heat treatment. The obtained samples have been observed by 3D scan, optical and scanning electron microscopies (SEM), and also microtomography.

The application of the slurry was done by spraying. After drying, irregularities in the topography and the microstructure appear depending on the spraying parameters.
In parallel, several non-destructive technics have been tested on the elaborated samples in order to find industrial adapted ones: terahertz waves, acoustic microscopy… The obtained results have been compared to microstructure analyse to validate them.

Keywords :

Ceramic matrix composites, environmental barrier coating, Non destructive control

[1] MBDA, BOURGES, FRANCE

Nomenclature

CMC – Ceramic Matrix Composites
CMO - Organic Matrix Composite
CMM - Metal Matrix Composite
EBC - Environmental Barrier Coating
NDT - Non destructive Test
LSI - Liquid Silicium Infiltration
Si - Silicium
SiC - silicon carbide
C/C - carbon / carbon
PDC - Polymer Derived Ceramic
THz - onde tera hertz
SEM - scanning electron microscopies

1. Introduction

The demands of governments are pushing industrialists to produce increasingly efficient and reliable vehicle. The need to go faster and higher requires the development of materials with ever more impressive characteristics, which were thought to be unattainable a few years ago. It is in this dynamic that Ceramic Matrix Composites (CMCs) were born. Today, to fully utilize their thermal capacity, it is not possible to use them raw. Different constraints require us to associate them with other materials to create a final product that is usable and efficient. The main flaw of CMCs is their oxidation in contact with oxygen at high temperature, to prevent the parts from disintegrating during use, they must be isolated from their external environment. This is why an environmental barrier coating (EBC) is applied to the surface of the parts.

The objective of this study is to analyze the application of the EBC on a CMC part to improve properties in the controls to be carried out to verify the conformity of the product with respect to the specifications.

To do this, first, the context of the study will be presented. Then, we will study the different control methods implemented. And finally, we will compare the different methods using the results obtained.

2. Context

This context will allow us to clearly define a CMC and their characteristics. Then, in a second step, the definition of an EBC will be specified, understand its usefulness and implement its application.

2.1. CMC

Like any composite, a CMC is a solid phase material, most often heterogeneous and anisotropic, composed of at least two constituents whose respective qualities complement each other to form a material with improved overall performance.
It consists of:

- A reinforcement, usually in the form of fibers or filaments, which governs most of the mechanical and thermomechanical properties (toughness, stiffness, resistance to breakage, etc.).
- A matrix, playing the role of binder, and allowing to protect the reinforcement from chemical or mechanical aggressions of the environment, to maintain it in its initial position and to ensure the transmission of efforts.
- An interface between the reinforcement and the matrix capable of deflecting cracks generated in the matrix to avoid the breakage of fibers or the matrix at the same place.

Ceramic matrix composites have the main characteristic of withstanding use at very high temperatures. Figure 1 shows that CMCs clearly surpass other types of composites such as CMO or CMM in temperature. The temperature properties of CMCs are mainly derived from the ceramic. This material is characterized by strong covalent bonds between atoms, increasing the melting temperature.

Depending on the atoms contained, an electromagnetic transparency of the material is possible and can be very useful for discreetly launching missiles on enemy bases. Finally, CMCs allow a significant weight reduction of between 30% and 40% compared to their metallic counterparts.

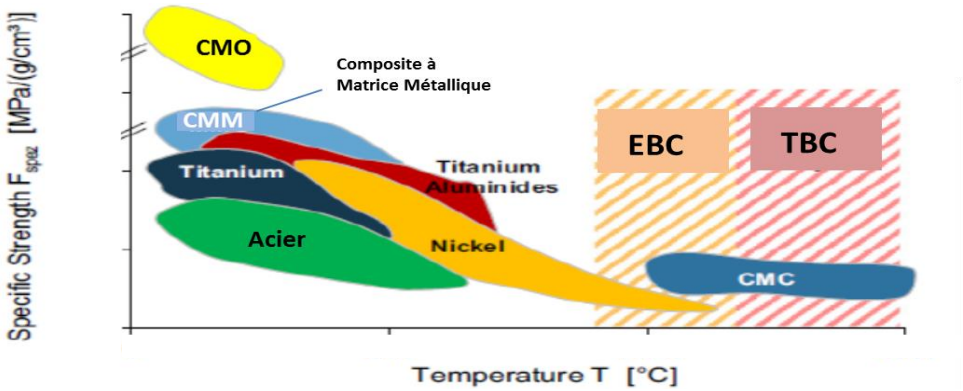

Fig 1. Specific strength as a function of temperature for different materials

However, during high-temperature use, CMCs are sensitive to oxidation. To make the best use of their capacity, it is necessary to protect them with an environmental barrier (EBC) [2].
We will now focus on this environmental barrier in the next chapter.

2.2. EBC

Figure 2 shows that the environmental barrier is deposited as a film on the CMC to protect it [1-2]For the environmental barrier to function optimally, perfect adhesion between the two materials is required. To achieve this, it is necessary to first have a controlled and adapted surface state of the CMC for the application of the environmental barrier. Secondly, the chemical interaction between the CMC and the environmental barrier must be optimal to ensure its proper functioning.

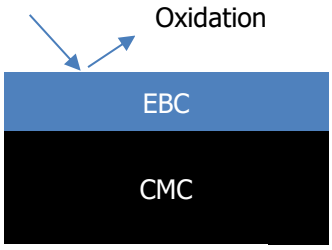

Figure 1. *EBC*

In our case, we will study an environmental barrier obtained by LSI (Liquid Silicon Infiltration). This process involves applying silicon to a carbon-based CMC to obtain SiC after reaction (equation 1) [1-3-4].

$$C_{(s)} + SI_{(l)} \xrightarrow{^{\circ}C} SIC_{(s)}$$

Equation 1 : Chemical reaction between carbon and silicon at high temperature

The application of this EBC is carried out in several steps. First, a product containing silicon particles is sprayed onto the preheated surfaces of the part to be treated. The coated part then undergoes a high-temperature thermal cycle during which the pyrocarbon matrix reacts with the molten silicon to form silicon carbide, resulting in the C/C-Si [5].

3. Non Destructive Test (NDT)

To determine the thickness of silicon deposited on the surface of the CMC, various NDT methods have been selected. These controls therefore make it possible to check the thickness of the product applied before sending the part for baking. In this section, we will present the different NDT methods used in this study.

3.1. Scan 3D

The 3D scan is a device for 3D scanning and acquisition that collects data on a physical object, including its shape and texture. The 3D scan uses lidar technology to scan the part and arrive at this reconstruction. In the case of this study to determine the thickness of the product, it will be necessary to perform a scan on the plate without the product to obtain a reference surface. In a second step, the scan will be performed on the plate with the slurry. The thickness of the product deposited will be determined by comparing the two scans. These thickness measurements of the slurry with the 3D scan method will serve as a reference to compare the values determined with the other NDT methods [9].

3.2. X-ray Nano tomography

X-ray tomography is a non-destructive technology used as an imaging technique to inspect internal and external structures of parts. Nano-tomography allows better quality images to perform finer analyses. The disadvantage of nano-tomography is the size of the samples or parts that can be processed, on the order of a few centimeters [10].

3.3. Terahertz waves (THz)

Terahertz waves have a strong penetrating power and can see through certain materials. This study will determine if these properties can be adapted to our need for measuring the thickness of the slurry deposit. Given the dielectric nature of this deposit, the implementation of a THz technique seems entirely appropriate. The purpose of this study is to confirm this.
The principle is that of a time-of-flight measurement, that is, a THz pulse is emitted towards the surface of the sample. When it passes through an interface, a fraction of it is reflected. Thus, the signal reflected by a multilayer sample is a train of pulses. The delay between two consecutive pulses provides information on the thickness of the corresponding layer. In our case, it is a single-layer coating, and we expect to observe 2 pulses with a delay directly related to the thickness of the layer [7 - 8].

3.4. Laser Photothermal Radiometry

The photothermal radiometry technology uses a laser diode to determine the thickness of the deposit layer by heating the material and detecting the re-emitted heat flow. This heat flow is related to the thickness of the substrate layer, but also to its thermophysical properties. Once the return heat flow is detected by the sensor, there is a calculation processing phase to obtain the value of the slurry layer thickness. This is a promising and fast-to-implement technology, ideal for considering use in production controls [6]

4. Results Presentation and Comparison of Methods

During this study, three different samples will be studied in order to compare the methods and to validate or not their reliability for measuring the thickness of the deposited slurry.

4.1. Presentation of samples

Three samples were taken from the same plate. This plate underwent three different product applications to obtain different thicknesses. Sample A corresponds to the area with the thickest deposit, while sample C corresponds to the area with the thinnest deposit.

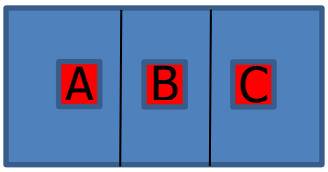

Figure 2 : *Sampling scheme for samples A-B-C*

The complete plate was scanned in 3D, and thickness results were obtained for the entire plate. These thickness values will serve as a reference for comparing the results.
Samples A-B-C underwent nanotomography and were tested using acoustic microscopy to see if the results by this method are reliable and repeatable.
Finally, sample 5 was tested using terahertz waves to validate the feasibility of the method.

4.2. Scan 3D

Figure 4 shows the result of the scan of our plate with the different thicknesses of slurry. The colour gradient represents the differences in thickness, with red indicating thicker areas and green indicating thinner areas, as shown on the colour scale. In the red zone, we find sample A, in the orange-yellow zone, we find sample B, and finally, in the green zone, we find sample C.

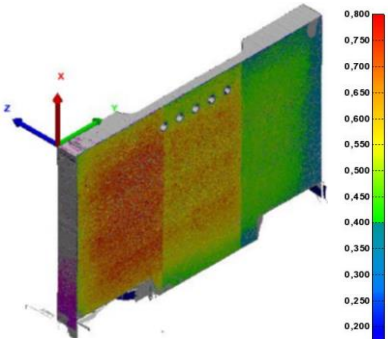

Figure 3 : *3D scan of the sampling plate*

Figure 5 shows a focus on the part of the plate with the thickest slurry layer. The measured thickness varies from 0.533 to 0.698 mm depending on the areas on the plate. It can be observed that the thickness is not the same at the edge of the plate as in the center. This is due to the application of the slurry. In our study, we are not interested in this phenomenon of inhomogeneity in the distribution of the slurry.
In the sampling area of our cube, we have a measured thickness of 0.68 mm.

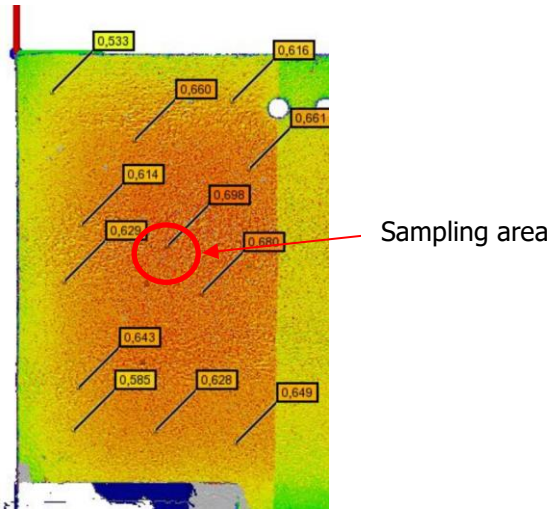

Figure 4 : *Zone from which sample A was taken*

Figure 6 shows a focus on the central area of the plate, where the thickness varies from 0.51 to 0.64 mm. The thickness value of the sample B is therefore 0.56 mm.

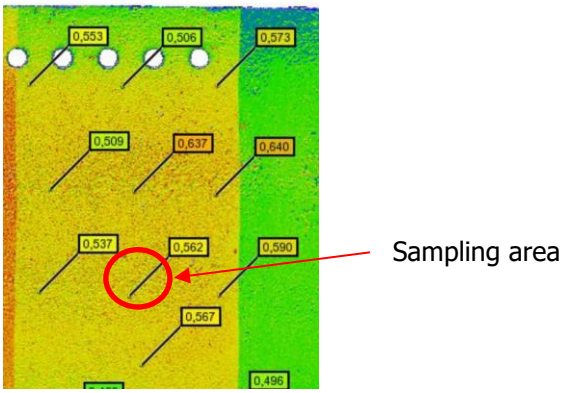

Figure 5 : *One from which sample B was taken*

Finally, for the 3D scan, Figure 7 shows a focus on the central area of the plate with the thinnest slurry layer. We have thickness variations of 0.411 to 0.448 mm. The thickness value of sample B is therefore 0.439 mm.

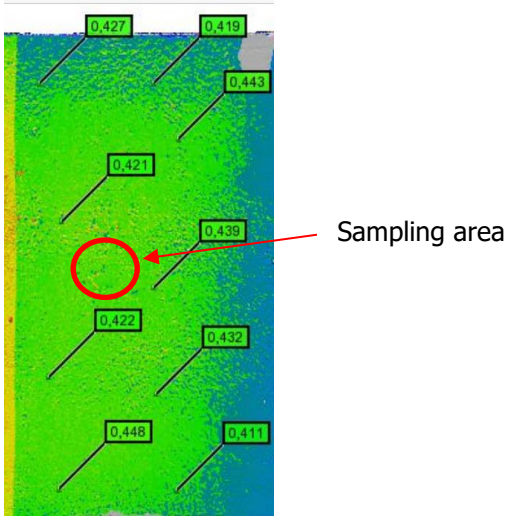

Figure 6 : One from which sample C was taken

Based on these initial results, we can validate the theory on layer thicknesses. Indeed, the thickness increases from aera A to area B (Table 1).

Sample	**A**	**B**	**C**
Thickness (mm)	0.68	0.56	0.44

Tableau 1 : Thickness of samples A-B-C with the 3D scanning method

4.3. X-ray Nano tomography

Figures 8-9-10 are nano-tomography images of the 3 samples. It can be observed that on such a fine analysis, the slurry is not distributed homogeneously on the CMC. This results in a high variability in the thickness measurement.
To reduce the error due to measurements and the inhomogeneity of the slurry, we determined the average thickness of each sample by taking the average of 6 measurements.
As can be observed in Figures 8-9-10, there is a clear separation between the CMC and the product, even if the contact surface between the two materials is not linear.

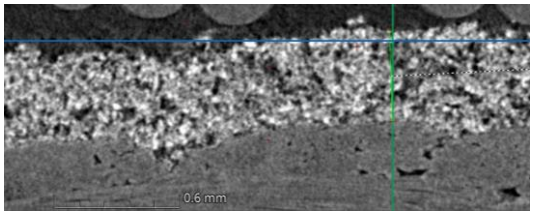

Figure 7 : View of a slice of sample A

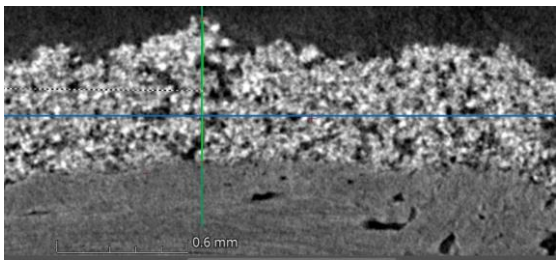

Figure 8 : View of a slice of sample B

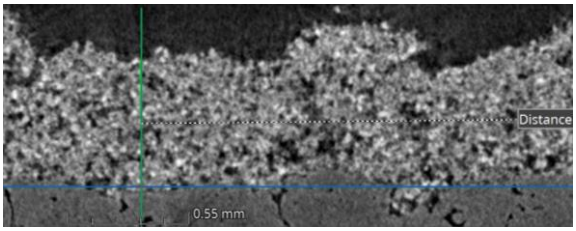

Figure 9 : View of a slice of sample C

Figures 8-9-10 show that the distribution of the slurry at the microscopic scale is inhomogeneous, this is confirmed by the thickness measurements in table 2.

Sample	Thickness reading (mm)						Average
A	0.58	0.67	0.45	0.63	0.53	0.72	**0.76**
B	0.58	0.72	0.61	0.60	0.79	0.79	**0.68**
C	0.44	0.43	0.37	0.48	0.47	0.44	**0.44**

Table 2 : Recording of the thicknesses of each sample using the nano tomography method

4.4. Laser Photothermal Radiometry

Before carrying out the tests, a repeatability test was performed (Figure 11). For this, 10 measurements were taken on the same point. This verification makes it possible to ensure that the results obtained for the slurry thicknesses of each sample are representative of reality.

REPETABILITE	Enovasense (µm)
Mesure 1	664,45
Mesure 2	663,08
Mesure 3	663,12
Mesure 4	663,68
Mesure 5	662,20
Mesure 6	662,35
Mesure 7	662,61
Mesure 8	663,16
Mesure 9	663,05
Mesure 10	663,24
Moyenne	663,09
Ecart-type	**0,65**

Figure 10 : Repeatability of the laser photothermal radiometry method

The results of the tests using the radiometric photothermal method are conclusive, as can be seen in Figure 12. The color scale gives an indication of the homogeneity of the slurry thickness, with lighter colors indicating a thicker slurry layer.

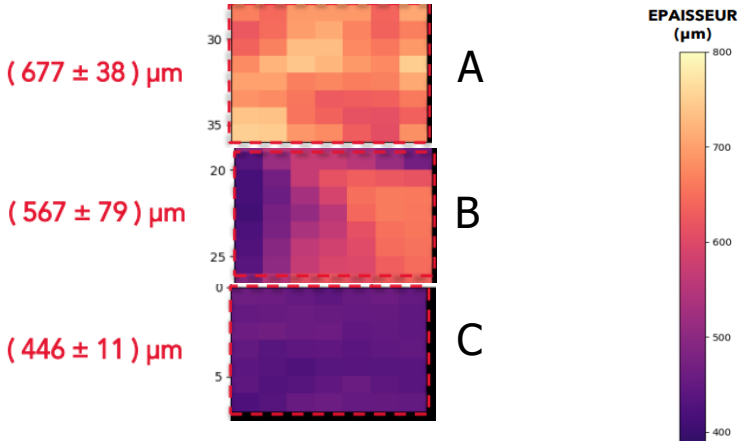

Figure 11 : Results of radiometric photothermal analysis

It can be observed that depending on the samples, the measurements do not have the same variability of results. This variability difference is due to the inhomogeneity of the slurry deposit.

Sample	**A**	**B**	**C**
Thickness (mm)	0.677	0.567	0.446
Variability (mm)	± 0.038	± 0.079	± 0.011

Tableau 3 : Measurement of the thickness of each sample with the photothermal radiometry method

4.5. Terahertz waves (THz)

The terahertz wave method was tested only on sample B. The objective was to verify the feasibility of this method to meet our needs.
In Figure 13, it is possible to observe the interfaces detected during the profile performed on sample B. On the raw measurement, the first interface corresponds to the reflection on the surface of the sample. It can be noted that the surface is not very regular due to surface roughness. We also observe further down (i.e. further in the time scale) the plate on which the sample was placed during the measurement. By increasing the contrast of this image, we observe here a second less intense line after the one corresponding to the first interface. We started by checking at what optical thickness it corresponded. The calculation of the average delay between these two lines on all measured points found an average optical coating thickness of 323 µm with a standard deviation of 23 µm. If this result is divided by a refractive index of 2, an average thickness of approximately 160 µm is obtained. This falls within the expected range of thicknesses.
The standard deviation can be explained by the high surface roughness. These roughness can have a significant impact on the measurement results of coating thickness because, due to the size of the wavelength (approximately 300 µm), the THz wave sent will be reflected in part on the peaks and troughs of the roughness, creating a "blur" on the real position of the interface. This will distort the estimation of the coating thickness. We therefore applied a filter to take into account only the low frequencies, allowing averaging over a larger sample surface but this is not sufficient for the roughness present on sample B. Moreover, if we go down too much in frequency, the measurement resolution becomes too low considering the expected range of thicknesses.

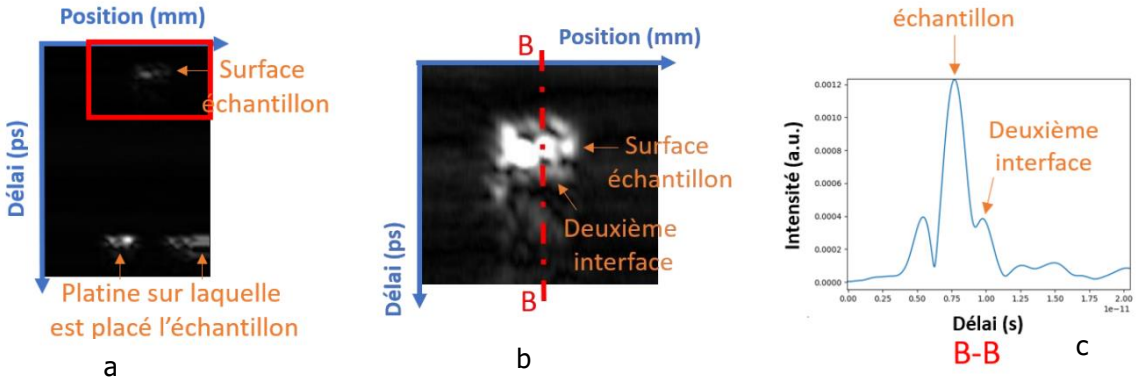

Figure 12 : Profile obtained on sample B, figure (a) corresponds to the raw data collected, figure (b) corresponds to the same profile but with increased contrast. We have zoomed in on the area of interest, framed in red. This allows to observe a second interface. Figure (c) is an example of an A-scan measured, along the red dashed line.

4.6. Comparison of results

If we take stock of the methods and results obtained in Table 4, based on a reference value obtained by 3D scan, we notice that the values obtained by 3D scan and radio photometry are very similar, within a few micrometers.
In nano-tomography, the results are distorted by the irregularity of the slurry layer. Tomography is not a reliable means of measuring an average thickness, but rather a thickness at a specific point.

As for the terahertz method, we see that the measurement is very different from the values measured with the other methods. This deviation is certainly due to porosity, the thin layer of slurry, and the lack of knowledge of the refractive index of the product in the THz domain. To obtain reliable results, more time would need to be spent adjusting the machine. However, this improvement remains a hypothesis, as the thin layers to be measured suggest that this measurement method may not necessarily be repeatable.

Sample	**A**	**B**	**C**
3D scan thickness (mm)	0.680	0.562	0.439
Nano tomography thickness (mm)	0.760	0.680	0.440
photothermal radiometry thickness (mm)	0.677	0.567	0.446
terahertz wave thickness	X	0.16	X

Tableau 4 : Summary of the thicknesses measured for each sample with each method

5. Conclusion

This study highlighted the importance of the environmental barrier for protecting our material. Indeed, without this protection, it is not possible to exploit all its mechanical and thermal properties. To ensure that this protection is effective, it is crucial that its application is controlled to meet specifications as closely as possible. One key parameter for controlling the process of applying the environmental barrier to the material is the thickness of the slurry that is deposited on the part before it is sent for baking.
It is important to determine a method for controlling the deposited thickness of the slurry without damaging the part. This study allowed us to compare four different methods to ensure their feasibility and reliability.
We saw that two control methods stand out. The 3D scan and photothermal radiometry methods give us equivalent, reliable, and repeatable results. On the other hand, the nano-tomography method is too precise for the measurement, given that the substrate is not applied homogeneously at the microscopic scale. Moreover, the size of the parts that can be passed through nano-tomography is a significant limitation. Finally, the terahertz wave method gives inconclusive results regarding our application.

References

1. A. Favrea , H. Fuzellierb, J. Suptil : An original way to investigate the siliconizing of carbon materials
2. R. Kochendörfer, N. Lützenburger : Applications of CMCs Made via the Liquid Silicon Infiltration (LSI) Technique
3. Martin Frieß , Matthias Scheiffele , Wolfgang Zankl , Frank Hofmann : Development, Manufacture and Characterization of C/C-SiC Components Based on Filament Winding
4. Thomas Reimer, Ivaylo Petkov, Dietmar Koch, Martin Frieß, Christoph Dellin : Fabrication and characterization of c/c-sic material made with pitch-based carbon fibers
5. O. DEZELLUS∗, S. JACQUES / F. HODAJ, N. EUSTATHOPOULOS : Wetting and infiltration of carbon by liquid silicon
6. Julien JUMEL : Microscopie Photothermique : Application à la Caractérisation des Propriétés Thermoélastiques Microscopiques de Composites Carbone/Carbone et de Barrières Thermique
7. Emmanuel HIDALGO , Contrôles non destructifs par terahertz de revêtements de forte épaisseur et détection de défauts aux interfaces (corrosion, décollements, …)
8. X.-C. Zhang , "Terahertz imaging and sensing for non-destructive testing and evaluation" published in Journal of Physics D: Applied Physics, 2005.
9. Y. Zhang Non-destructive thickness measurement of coatings using structured light 3D scanning", published in Measurement , 2019
10. F. De Carlo, X-ray Nanotomography: High-Resolution 3D Imaging of Materials and Life Sciences Samples